

Dynamic Response of a Combined Spar-Type FOWT and OWC-WEC by a Simplified Approach

A. Abazari*

Chabahar Maritime University, Chabahar, Iran.

Received Date 19 March 2022; Revised Date 02 April 2022; Accepted Date 12 April 2022

* Corresponding author: abuzarabazari@cmu.ac.ir, abuzarabazari@yahoo.com (A. Abazari)

Abstract

A combination of offshore wind turbines and wave energy converters has recently been the focus of the researchers. Many types of converters have been installed on the offshore platform in the design step, and the performance of these hybrid systems has been investigated. The oscillating water column converter is one of the most favorite and commercialized systems due to its efficiency and low maintenance cost. In the present work, a new design including the array of the oscillating water column in a circular arrangement around the spar-type platform is considered. The coupled governing equations are solved based on the simplified analytical approach through the frequency domain analysis. The results obtained show that the increase in the number of energy converters increases the total generated power, and consequently, the converters capture the vibrational energy of the spar platform. Therefore, the dynamic response of the spar decreases in the case with an array of energy converters, which is one of the main objects of this hybrid system.

Keywords: *Oscillating water column, wave energy converter, offshore wind turbine, frequency domain analysis.*

1. Introduction

An ocean has two types of energy resources. These are waves and wind for producing electricity [1]. The development of offshore wind turbines and wave energy converters (WECs) should not disorganize the ecological balance [2]. Therefore, due to the efficient use of natural resources and the reduction of the costs for a feasible project, considering the strong synergies and integration of floating offshore wind turbines (FOWTs) and WECs is necessary. Recently, combining WECs with offshore wind turbine (OWT) farms has been the researchers' focus, which has some advantages such as increasing the overall efficiency and reducing the dynamic response of the floating platforms. It has just been mentioned that these structures are large-scale energy harvesters for industrial applications, while there are several other approaches to energy harvesting on a small scale for low-powered devices [3, 4], which are not the scope of this study.

Different types of hybrid systems of OWT and WEC have been studied by the researchers, as follow:

There are studies about combining the point absorber WECS with OWT. A hybrid WEC point absorber attached at the center of the wind float has been investigated by Peiffer *et al.* [5]. Muliawan *et al.* [6] have suggested a Spar-Torus Combination (STC) system combining a spar-type floating wind turbine with a point absorber WEC (Wavebob). The point absorber slides along the spar length to harvest the wave power. STC showed a lower vibration and more power output than the single spar. Bachynski and Moan have analyzed a combined system of an OWT on a single column tension leg platform and 3 point absorber WECs numerically [7]. Two assumptions of the purely heave motion relative to the tension leg platform (TLP) hull and a hinged body moving in coupled surge and pitch, as well as heave, were considered. Hanssen *et al.* have tested a W2Power hybrid offshore wind turbine and an array of point absorber WEC in a large but lightweight semi-submersible floating platform. They presented an economic performance analysis [8]. Chen *et al.* have experimentally evaluated the performance of the key components of a hybrid system including a wind wheel with a

hemispherical oscillating body responsible for capturing the energy from the irregular wind and waves [9]. Karimirad and Koushan have assessed the dynamic response and power production numerically in an operational condition for a spar-type OWT and oscillating buoy WEC. They considered a coupled aero-hydro-servo-elastic time-domain dynamic simulation. They showed that tuning of the power-take-off system could improve the power performance [10]. Kluger *et al.* [11] have utilized a simplified method for modeling the dynamic of spar type OWT and WEC using linear, steady-state, long-wave approximations. They used three types of WECs including surge-mode internal surge tuned mass damper, heave-mode internal tuned mass damper, and heave-mode external WEC in their study. Wang *et al.* [12] have evaluated the hydrodynamic performance and energy production of a combined 5-MW semi-submersible OWT with a heave-type WEC installed on the central column of the platform. They numerically studied the effect of the power take-off (PTO) system parameters on output power. Patil and Karmakar have evaluated the hydrodynamic performance of spar type OWT combined with four and six cone-cylindrical-shaped heaving type point absorber numerically [13]. The results obtained showed that spar stability was improved by the array of WECs. Michailides [14] has assessed the hydrodynamic response and the produced power of combined spar type OWT with different configurations of oscillating buoy WEC. Their approach was based on the generalized modes considering the wave-structure interaction. They found that the small space between the spar and WECs caused a strong interaction, and consequently, decreased the produced power.

The flap-type surge WEC has also been combined with OWT. Peiffer and Roddier have examined the performance of an integrated oscillating wave surge converter with a wind float structure numerically and experimentally. The system consists of three hinged flaps oscillating rotationally about the main beams of the platform. They found that the proposed integration could improve the overall economics [15]. Similarly, a flap-type WEC combined with a semi-submersible floating OWT was studied by Luan *et al.* [16] for evaluating the power production and power cost reduction. They showed that the PTO damping coefficient and the cylinder mass significantly affected the output power.

The oscillating water column (OWC) WECs work based on the output flow rate crossing a well

turbine that is combined with OWT. Aubault *et al.* have used an OWC WEC incorporated into the wind float hull [17]. They concluded that this design enhanced the economic cost due to sharing of both the mooring system and power infrastructure. O'Sullivan has also analyzed a combined multi-Mega-Watt wind turbine platform with a Delta OWC Array [18]. Perez-Collazo *et al.* have investigated the feasibility of a combined OWC WEC with an OWT on a monopile structure [19]. They experimentally tested the 1:37.5 scale model of the proposed system under regular and irregular waves. This was similar to the concept presented by As Perez and Iglesias [20] for offshore windmills. Perez-Collazo *et al.* have also proposed a combined system including the oscillating water column WEC with an offshore wind turbine on a jacket platform. They experimentally tested a 1:50 scale model under regular and irregular waves to find the hydrodynamic response of the WEC sub-system. They confirmed that this concept worked well [21].

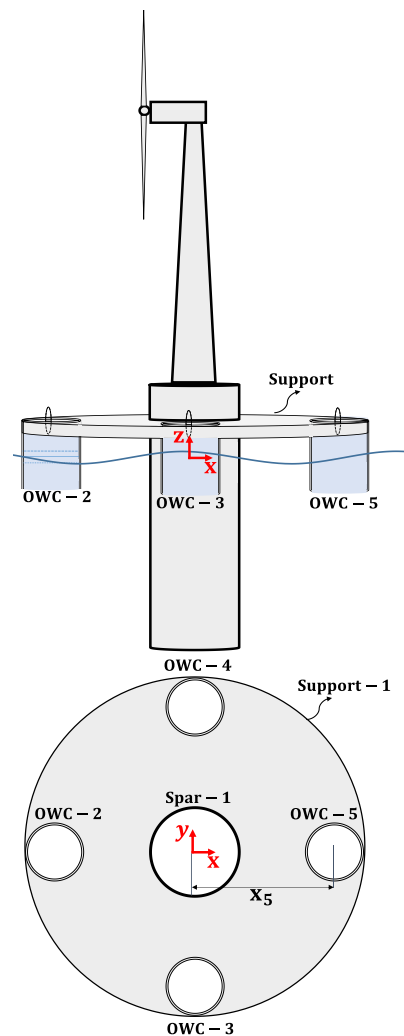


Figure 1. Combined OWT with four OWC WECs.

OWC WECs, due to the few mechanical parts and low cost of the manufacturing and maintenance issues, have been widely commercialized. The previous studies for combined OWC and OWT are related to a specified design in which OWC WEC is mounted around the main column of the spar platform. In the present work, the new suggested design is the array of OWC WECs mounted on a circular support attached to the spar column, as in figure 1. It is noted that the supports can also be a truss structure. The subscript of OWC, in figure 1, starting from 2, is related to the degrees of freedom, which is explained more in the next section.

On the other hand, an analytical and generic simplified method can be used for the mathematical modeling of the dynamic response of integrated OWC and OWT. Such methods are helpful for the early stage of a project to approximately estimate the desired output overall. Therefore, the paper is organized as what follows. First, the characteristic values of the considered case study are introduced. Secondly, the mathematical model of the dynamic response of the combined OWT and OWC WEC is developed. Finally, the effects of OWC WEC on the platform's generated power and hydrodynamic response are discussed.

2. Mathematical Model

A simplified rigid piston model can express the mathematical model of an OWC. The motion equation can be simulated as a vibrational system with a single degree of freedom if the chamber is fixed; otherwise, in the condition of a floating chamber for an OWC WEC, the equivalent vibrational system is two degrees of freedom. The heave motion of the floating part and piston-like reciprocating motion of the water column is not the same as such causes an equation system with two degrees of freedom. It is noted that the linear airy wave theory, based on the assumption of incompressible and irrotational flow, is utilized to simulate the wave.

If the dimension of the OWC chamber in the wave direction is small compared to the wavelength, the heave motion of the water-free surface inside the chamber is a correct assumption [7-10]. This reciprocating motion is the response of floating OWC with two degrees of freedom due to the wave excitation force. In a single floating OWC WEC, the buoyancy and assigned draft should be created by the buoyant volume mounted around the chamber in order to overcome the OWC weight. However, for the suggested hybrid system, the weight of the OWC arrays compared

to the spar platform is negligible, and the spar draft dictates the chamber draft due to the rigid connection between the chambers and the platform. Therefore, there is no need to design a buoyant object around the chamber.

The dynamic motion of the present hybrid structure is a little different. When the OWC chambers are attached to the spar platform through the support, as in

Figure 1, the heave motion of the spar platform, support, and all OWC chambers have the same displacement. This is based on the assumption that the coupling between pitch and heave is neglected, and the spar pitch motion does not cause the difference between the heave motion of the OWC chambers around the support. On the other hand, the heave displacement of the water-free surface inside OWC is free from the spar heave displacement. Hence, the dynamic motion of the spar and four OWC WECs can be interpreted as a vibrational heave system with five degrees of freedom by neglecting the coupling with other directions. The Newton's second law is used to introduce the dynamic motion in the heave direction as equation (1) just for the main part (spar, support, and OWC chambers) of the system. Since subscript 1 is related to the first degree of freedom for the main part, consequently, for the remaining degrees of freedom as the free surface motion of four OWC WECs, the subscript number is 2 up to 5.

$$\left(M_{spar} + M_{support} + \sum_{j=2}^5 M_{tube,j} \right) \ddot{z}_1 = f_{fr-spar} + \sum_{j=2}^5 f_{fr-tube,j} + f_{dif-spar} + \sum_{j=2}^5 f_{dif-tube,j} + f_{r-spar} + \sum_{j=2}^5 f_{r-tube,j} + f_{vis-spar,tubes} + f_{hstat-spar} + \sum_{j=2}^5 f_{hstat-tube,j} + \sum_{j=2}^5 f_{air-tube,j} \quad (1)$$

$$f_{air-tube,j} = +S_j \cdot p_{a,j} \quad (2)$$

where M_{spar} , $M_{support}$, and $M_{tube,j}$ are the mass of spar, support, and OWC tubes. $f_{fr-spar}$ and $f_{fr-tube,j}$ are the Froude-Krylov incident wave force applied on spar and OWC tubes. $f_{dif-spar}$ and $f_{dif-tube,j}$ are the wave diffraction force applied on the spar and OWC tubes. f_{r-spar} and $f_{r-tube,j}$ are wave radiation force applied on spar and OWC tubes. $f_{vis-spar,tubes}$ is the viscose friction force applied

on the spar and OWC tubes. $f_{hstat-spar}$ and $f_{hstat-tube,j}$ are the hydrostatic force applied on the spar and OWC tubes. $f_{air-tube,j}$ is the force imposing from the compressed air pressure above the free surface level applied on the tube, and consequently, on the spar platform, as in equation (2). $p_{a,j}$ is the air pressure.

It is noted that since we have five degrees of freedom, one for the platform and four degrees for OWC water-free surface level, and due to the assigned first number of the degree of freedom for the platform, the number of OWC starts from 2. By this assumption, the assigned number of degrees of freedom for each OWC is the same as the number of OWC.

- Z_1 for the spar, support, and tube
- Z_2 for OWC2
- Z_3 for OWC3
- Z_4 for OWC4
- Z_5 for OWC5

Therefore, j is a number between 2 and 5, which is related to the degree of freedom of the water-free surface inside each OWC WEC. S_j is the surface area of the water column of each OWC WEC.

Now, the dynamic motion of the piston model of an OWC WEC is expressed as in equation (3). It is worth noting that the mentioned equation is four independent equations assigned to each OWC WEC.

$$M_{WC,j}\ddot{Z}_j = f_{fr-WC,j} + f_{r-WC,j} + f_{hstat-WC,j} + f_{air-WC,j} \quad j = 2,3,4,5 \quad (3)$$

$$f_{air-WC,j} = F_{air-WC,j}e^{i\omega t} = -S_j \cdot p_{a,j} = -f_{air-tube,j} \quad (4)$$

where $M_{WC,j}$, $f_{fr-WC,j}$, $f_{r-WC,j}$, $f_{hstat-WC,j}$, and $f_{air-WC,j}$ are the water column mass, Froud Krylov, radiation hydrostatic, and pressurized air forces applied on the water column in each OWC WEC. All the equations (1) to (4) are approximated to be linear so that a frequency domain analysis of the equation of the motion with 5 degrees of freedom can be applied.

The crucial part of Equations (2) and (3) being responsible for the coupling of the equations is the air pressurized force. By assumptions as the linearity of the equations, air to be as an ideal gas, the isentropic process for the air compression, the spring-like effect of air compressibility, and the linear relation between the mass flow rate and the pressure difference [22-24], the air pressure and flow rate for each OWC WEC is developed as:

$$p_{a,j} = P_j e^{i\omega t} \quad , j=2:5 \quad (5)$$

$$P_j = \left[\left(\frac{K_j D_{wc,j}}{N} + i\omega \frac{V_{0,j}}{C^2} \right)^{-1} \rho_a \right] Q_j = [\Lambda] Q_j; j=2:5 \quad (6)$$

$$Q_j = -i\omega S_j (Z_1 - Z_j) \quad ; j=2:5 \quad (7)$$

P_j and Q_j are the pressure and flow rate amplitude. K_j , $D_{wc,j}$ and N are the constant, diameter, and rotational speed of the turbine. $V_{0,j}$, C , ρ_a , and ω are air volume, sound speed, air density, and wave frequency, respectively. Z_1, Z_j are the heave displacement of the spar and free surface level of each OWC WEC, respectively. Consequently, the air force is expressed as:

$$\begin{aligned} F_{air-tube,j} &= +S_j \cdot P_j = S_j \cdot \Lambda \cdot Q_j \\ &= S_j \cdot \left(\frac{K_j D_{wc,j}}{N} + i\omega \frac{V_{0,j}}{C^2} \right)^{-1} \rho_a \cdot (-i\omega S_j (Z_1 - Z_j)) \end{aligned} \quad (8)$$

After manipulation and simplification of the formulas, the coefficient of $-\omega^2 Z_j$ is separated and interpreted as the virtual mass of the turbine, $m_{Turb,j}$, and the coefficient of $\omega i Z_j$ is defined as turbine damping, $B_{Turb,j}$ that are introduced in equations (9) and (10):

$$B_{Turb,j} = \frac{S_j^2 \frac{K_j D_{wc,j}}{N} \rho_a}{\left(\frac{K_j D_{wc,j}}{N} \right)^2 + \left(\frac{\omega V_{0,j}}{C^2} \right)^2} \quad (9)$$

$$m_{Turb,j} = -\frac{\frac{S_j^2 V_{0,j}}{C^2} \rho_a}{\left(\frac{K_j D_{wc,j}}{N} \right)^2 + \left(\frac{\omega V_{0,j}}{C^2} \right)^2} \quad (10)$$

It should be pointed out that the parameters of S_j , $D_{wc,j}$, $V_{0,j}$, and K_j for each OWC WECs in the present study are considered the same.

Therefore, the air force can be stated in a simplified form only versus the defined parameters of $m_{Turb,j}$ and $B_{Turb,j}$ as below.

$$F_{air-tube,j} = (\omega i B_{Turb,j} - m_{Turb,j} \omega^2) Z_j + (-\omega i B_{Turb,j} + m_{Turb,j} \omega^2) Z_1 \quad , j = 2:5 \quad (11)$$

$$F_{air-wc,j} = (-\omega i B_{Turb,j} + m_{Turb,j} \omega^2) Z_j + (+\omega i B_{Turb,j} - m_{Turb,j} \omega^2) Z_1 \quad , j = 2:5 \quad (12)$$

A frequency-domain analysis can be used since the equations are approximated in the linear form. Hence, the equations are expressed versus the amplitude of the motion of each degree of freedom, $Z_{j=1:5}$. Therefore equations (13) and (14) are the frequency domain forms of equations (1) and (3), respectively, which have been rearranged. It is noted that radiation, viscose, and hydrostatic forces are defined in a linear form

versus the added mass, radiation damping, viscose damping, and hydrostatic stiffness coefficients.

$$\begin{aligned} &[-(M_{spar} + m_{a-spar} + \sum_{j=2}^5 (M_{tube,j} + m_{a-tube,j} + m_{Turb,j})) + M_{support})\omega^2 + \\ &(B_{r-spar} + B_{vis-spar} + \sum_{j=2}^5 (B_{r-tube,j} + B_{Turb,j}))i\omega + \\ &(C_{hstat-spar} + \sum_{j=2}^5 C_{hstat-tube,j})Z_1 + \\ &\sum_{j=2}^5 [(-\omega i B_{Turb,j} + m_{Turb,j}\omega^2)]Z_j = \\ &F_{fr-spar} + \sum_{j=2}^5 F_{fr-tube,j} + F_{dif-spar} + \\ &\sum_{j=2}^5 F_{dif-tube,j} \end{aligned} \quad (13)$$

$$\begin{aligned} &[+m_{Turb,j}\omega^2 - \omega i B_{Turb,j}]Z_1 \\ &+ [-(M_{WC,j} + m_{a-WC,j} + m_{Turb,j})\omega^2 \\ &+ \omega i (B_{Turb,j} + B_{r-WC,j}) + C_{hstat-WC}]Z_j \\ &= F_{fr-WC,j} \quad j = 2,3,4,5 \end{aligned} \quad (14)$$

The terms on the right-hand side of equations (13) and (14) are the corresponding amplitude of the wave excitation forces in equations (1) and (3), which are introduced with the first capital letter. By rearranging equations (13) and (14), a simplified form is achieved as equation (15).

$$\begin{aligned} &A_{11} \times Z_1 + A_{12} \times Z_2 + A_{13} \times Z_3 + A_{14} \times \\ &Z_4 + A_{15} \times Z_5 = F_1 \\ &A_{21} \times Z_1 + A_{22} \times Z_2 = F_2 \\ &A_{31} \times Z_1 + A_{33} \times Z_3 = F_3 \\ &A_{41} \times Z_1 + A_{44} \times Z_4 = F_4 \\ &A_{51} \times Z_1 + A_{55} \times Z_5 = F_5 \end{aligned} \quad (15)$$

where A_{jm} ($j, m = 1:5$) are the coefficients of the displacement amplitude after rearranging the equations. For instance, A_{12} is expressed as the form of $[+m_{Turb,2}\omega^2 - \omega i B_{Turb,2}]$. The other coefficients can be derived in a similar method. The force amplitude F_j ($j = 1:5$) on the right-hand side is introduced as equation (16).

$$\begin{aligned} &F_1 = F_{fr-spar} + \sum_{j=2}^5 F_{fr-tube,j} + F_{dif-spar} + \\ &\sum_{j=2}^5 F_{dif-tube,j} \\ &F_j = F_{fr-WC,j} \quad j = 2,3,4,5 \end{aligned} \quad (16)$$

These equations can be stated in the matrix form for simplicity as equation (17).

$$\begin{bmatrix} A_{11} & A_{12} & A_{13} & A_{14} & A_{15} \\ A_{21} & A_{22} & 0 & 0 & 0 \\ A_{31} & 0 & A_{33} & 0 & 0 \\ A_{41} & 0 & 0 & A_{44} & 0 \\ A_{51} & 0 & 0 & 0 & A_{55} \end{bmatrix} \times \begin{bmatrix} Z_1 \\ Z_2 \\ Z_3 \\ Z_4 \\ Z_5 \end{bmatrix} = \begin{bmatrix} F_1 \\ F_2 \\ F_3 \\ F_4 \\ F_5 \end{bmatrix} \quad (17)$$

$$\Rightarrow [A] \times [\bar{Z}] = [\bar{F}] \text{ or } A_{jm} \times \bar{Z}_{m,1} = \bar{F}_{j,1}$$

By assumption of the linear wave theory [25], the surface elevation of the wave is defined as:

$$\eta_{wave} = \frac{H}{2} \cos(kx - \omega t) \quad (18)$$

in which k is the wavenumber. The applied wave scattering force including the Froude-Krylov and diffraction parts on the spar, is expressed as [26]:

$$\begin{aligned} &F_{fr-spar} + F_{dif-spar} \\ &= \left[\eta_{wave} \cdot S_{spar} \cdot \rho_w \cdot g \cdot \frac{\cosh(k(h - d_{spar}))}{\cosh(kh)} \right. \\ &\quad \left. - \omega^2 m_{a-spar} \eta_{wave} \frac{\sinh(k(h - d_{spar}))}{\sinh(kh)} \right] \\ &\times \text{real}(e^{i(kx_1 - \omega t)}) \end{aligned} \quad (19)$$

where S_{spar} , d_{spar} , x_1 , and a_{33} are the surface area, draft, horizontal position, and heave acceleration of water particles, respectively. A similar concept can be applied for deriving the scattering force on the water column. Furthermore, the force applied to the floating part of the OWC tube is assumed to be related to a real parameter. It is equivalent to the area ratio of the OWC opening to the total base area of the floating OWC WEC [27]. The different values for the coefficients of the wavenumber, x_j , are responsible for the phase difference between the scattering forces applied on the spar, water column, and tubes.

There are some assumptions in the present study behind the development of the formulas. Due to this, we can have an easy solution for the governing equations. However, these simplifications are in good agreement with the real conditions, as many researchers confirmed those in the previously published papers that are as follows:

It should be noted that the proposed diffraction term in equation (19) is just an approximation due to the long-wave approximation ($D/\lambda < 0.2$). The diffraction force is overly small compared to the Froud Krylove force by the considered dimension of the system and wave characteristic values. The heave added mass of a semi-infinite spar cylinder was reported as $2.064\rho_w r_{spar}^2$ [28]. The radiation damping of the spar is neglected compared to viscose damping. The added mass and radiation damping of the water column in the present study is derived based on an analytical approach presented by Evan [29]. Moreover, the interaction between the OWC tubes and spar platforms are neglected. However, this interaction should be considered in a real condition when the space between the OWC and spar platforms are small. Finally, the hydrodynamic response of the system as the amplitude of each degree of freedom is derived as equation (20).

$$[\bar{Z}] = [A]^{-1} \times [\bar{F}] \quad (20)$$

3. Output Power

After deriving the displacement of the spar and free surface level of each OWC through equation (20), the complex amplitude of flow rate and pressure is calculated based on equations (6) and (7). Therefore, the averaged output power, $\overline{P_{o,j}}$ related to each OWC is computed as below:

$$\overline{P_{o,j}} = \frac{1}{T} \int_0^T \text{Real}(Q_j e^{i\omega t}) \times \text{Real}(P_j e^{i\omega t}) dt \quad (21)$$

$$j = 2:5$$

4. Case study

The characteristic values of the OWC WEC, spar platform, and excitation wave are presented in table 1, table 2, and table 3. This data is utilized for the solution of the governing equations. It is noted that the considered spar characteristic is approximately similar to the industrial NREL 5MW wind turbine [30], and the data for an industrial OWC and water wave is in the same range as the existed ones in some references [31, 32]. The considered constant damping ratio values are just an estimation not to derive a very large and unreal dynamic response at resonance.

Table 1. Characteristic values of OWC.

Parameter	Description	Value	Unit
N	Turbine rotational speed	100	Rad/s
D	Turbine diameter	1.75	m
K	Turbine flow/Pressure constant	0.28	...
ρ_a	Air density	1.25	Kg/m ³
$d_{chamber}$	OWC front wall draught	6-14	m
F_b	OWC freeboard	5	m
D_{wc}	Chamber diameter	2-6	m
$x_{j=2:5}$	Horizontal location of OWC	-9.75, 0, 0, +9.75 -10.75, 0, 0, +10.75 -11.75, 0, 0, +11.75	m
ζ	Viscose damping ratio of each OWC	0.04	
t_{tube}	Thickness of OWC tube	0.05	m

Table 2. Characteristic values of wave.

Parameter	Description	Value	Unit
ρ_w	Water density	1025	Kg/m ³
h	Water depth	320	m
ω	Wave frequency	0-1.8	Rad/s
H	Wave height	1	m

Table 3. Characteristic values of spar.

Parameter	Description	Value	Unit
d_{spar}	Draft of spar	120	m
M_{spar}	Spar mass, including ballast	$8e^6$	kg
$M_{support}$	Support mass	$4e^4$	kg
$D_{spar-MWL}$	Diameter at MWL	6.5	m
$D_{spar-bottom}$	Diameter at bottom	9.5	m
$x_1 = x_{spar}$	The horizontal location of OWC	0	m
ζ	The viscose damping ratio of the spar, tube, and support	0.04	

5. Results and Discussion

One of the objectives of the present work is to investigate how OWC WECs can affect the dynamic response of the platform, and how much power can be generated via these WECs. The four cases are considered as below, with $D_{wc} = 6$ m.

- 1) spar platform with four OWC-2,3,4,5 WECs
- 2) spar platform with two active OWC-2,5 WECs
- 3) spar platform with two active OWC-3,4 WECs
- 4) spar platform without any OWC WECs

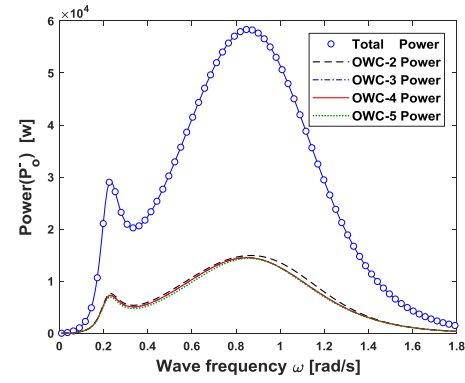
In cases 2, 3, and 4, which do not have some active OWC WECs, the damping and virtual mass of those inactive OWC turbines are considered to be a zero value such that the energy conversion cannot be created. It means that the system's structure including four OWC tubes, support, their weight, and the related excitation scattering force is the same in all four case studies. This issue is related to the fact that the comparison should be conducted in the same conditions, and only the energy conversion parts of each OWC have the main contribution to the heave displacement of the spar platform.

Figure 2 and figure 3 show that adding a large number of OWC WECs increases the total output power and decreases the spar platform's vibrational energy. This causes a lower heave displacement for the spar platforms with a larger number of OWC WECs compared to the cases with a small number of OWC WECs. Furthermore, it is demonstrated that although the location of OWC-2,5 is different from OWC-3, 4, the total output power and heave displacement of the spar platform in cases 2 and 3 are the same as in Figure 2-b,c, and Figure 3-b,c. This is related to the independence of the tubes' excitation forces on the OWC tubes' location. It is noted that the location of OWC-2,5 is at a negative and positive value of x or the left hand and right-hand side of the OWT, while OWC-3,4 are in $x = 0$.

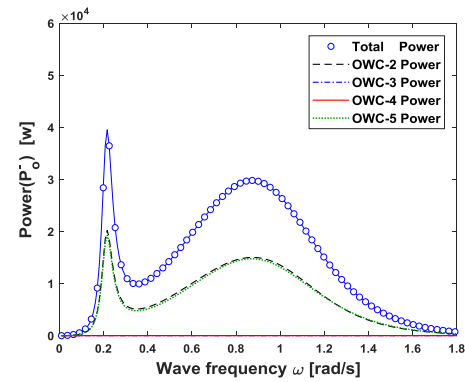
It is concluded from Figure 3-b,c that the free surface level of the water column inside of the inactive OWC is more than in the cases with active OWC WECs. Meanwhile, the assigned power for OWC WECs of 3, 4 in case b with active OWC WECs of 2, 5 is zero, which is vice versa in case c, as depicted in Figure 3-b,c. The other point is that the different location of case b and c is responsible for the different phase of the applied wave excitation forces in time-domain analysis. However, the frequency domain analysis's significant factor affecting the spar response amplitude operator (RAO) is the wave force amplitudes on OWC WECs that are not related to the OWC location. Therefore, the dynamic characteristic and the averaged captured power of case b with active OWC-2,5 is the same as case c with active OWC-3,4. This causes the spar RAO response to be the same for cases b and c, as shown in Figure 3-b,c. The purpose of the active OWC is related to the turbine's existence inducing the damping and virtual mass. On the other hand, an inactive OWC is like a hollow chamber with the open-top condition, in which the turbine does not exist such that there is not any resistance applied to the output flow rate. Consequently, the induced turbine damping and virtual mass should be zero in the equations.

The chamber diameter of an OWC WEC is the other key factor influencing the spar platform's output power and dynamic response. Therefore, the effect of this parameter is studied here. All the considered cases of hybrid OWT and OWC WECs include four OWC WECs with different chamber diameters. Figure 4 indicates that the cases with larger chamber volumes create more induced output power. On the other hand, a larger oscillation for both the spar platform and the water-free surface level is observed for the cases with smaller chamber diameters, as depicted in figure 5.

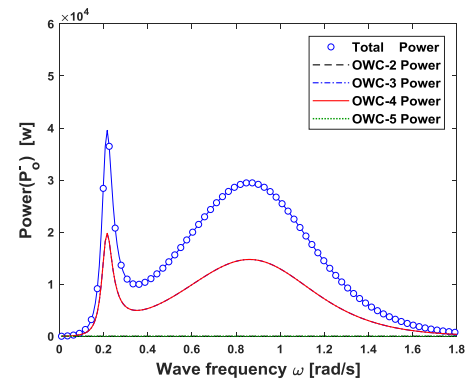
It should be emphasized that it is observed from figure 2 up to figure 5 that there are two peaks in all curves demonstrating the variation of the power and dynamic response of the hybrid systems versus frequency. The first peak is close to the natural frequency of the spar platform, which affects the coupled response of the free surface level of the OWC, and the second one is close to the natural frequency of the OWC free surface level. It is noted that in a fixed OWC WEC, one peak is only observed. As mentioned, the observed two peaks result from the coupled equations of the OWC WECs and spar platform.



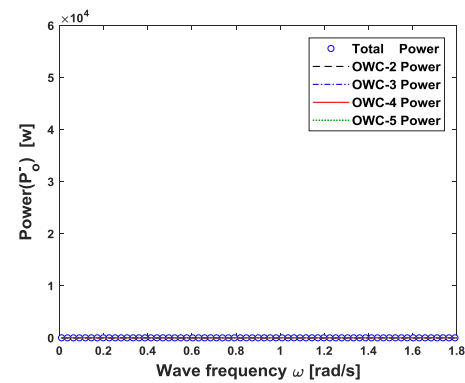
a) with four active OWC-2,3,4,5



b) with two active OWC-2,5



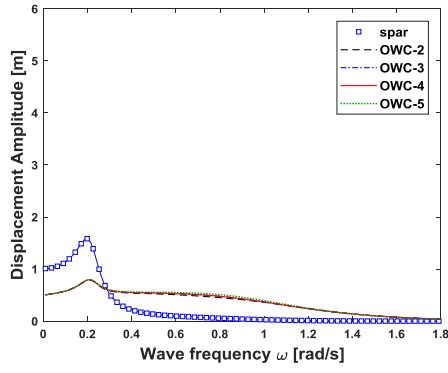
c) with two active OWC-3,4



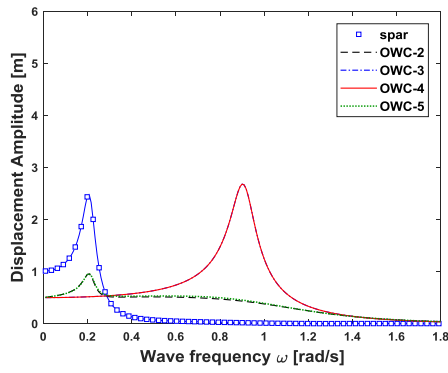
d) without OWC generated power

Figure 2. Generated output for combined OWT and OWC cases.

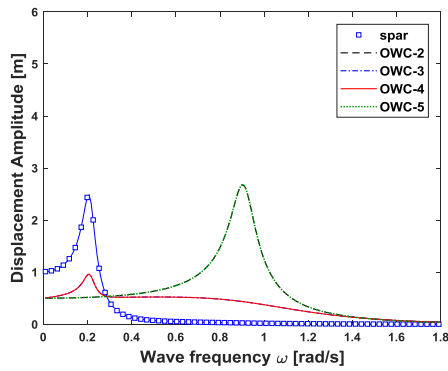
$$D_{wc} = 6 \text{ m}$$



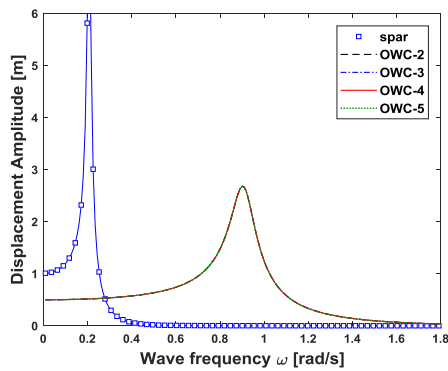
a) with four active OWC-2,3,4,5



b) with two active OWC-2,5

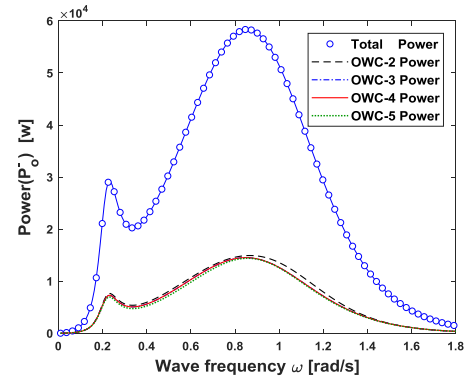


c) with two active OWC-3,4

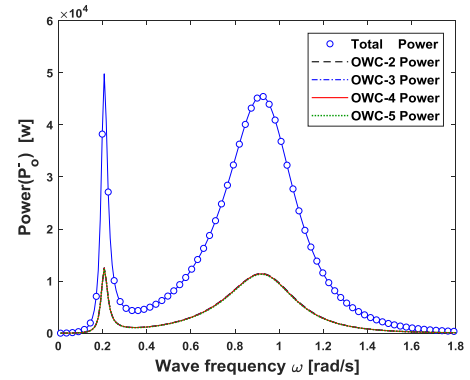


d) without OWC generated power

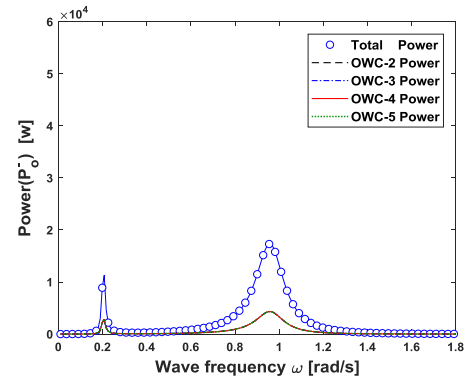
Figure 3. Resulted displacement of spar and free surface level for cases with $D_{wc} = 6\text{ m}$



a) $D_{wc} = 6\text{ m}$

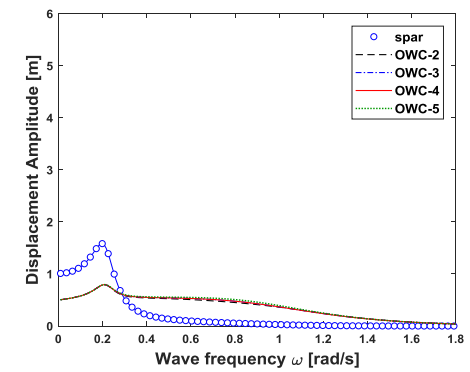


b) $D_{wc} = 4\text{ m}$



c) $D_{wc} = 2\text{ m}$

Figure 4. Generated output for different diameters for combined OWT with four active OWC.



a) $D_{wc} = 6\text{ m}$

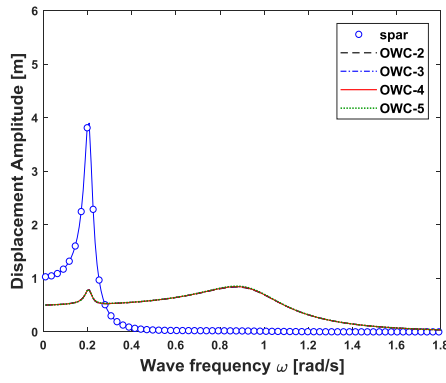
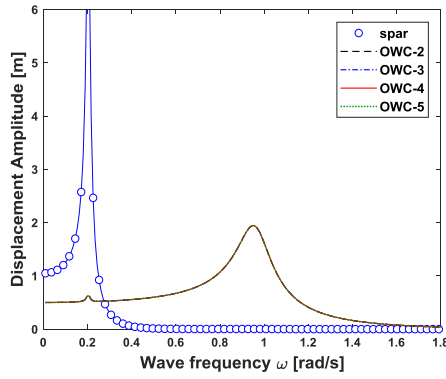
b) $D_{wc} = 4 \text{ m}$ c) $D_{wc} = 2 \text{ m}$

Figure 5. Resulted displacement of spar and free surface level for combined OWT with four active OWC.

In order to better understand the effect of the OWC's number and the influence of chamber diameter on the spar dynamic response, the heave RAO of the spar is presented in figure 6 and figure 7. The results obtained show the considerable effects of both the OWC WEC number and chamber diameter on reducing the spar heave RAO response. The increase in the number of the OWC WECs enhances the captured vibrational energy of the combined system, and hence, the spar vibrational energy and dynamic response decrease. On the other hand, as it is evident from equations 9 and 10, the turbine virtual mass and damping are dependent on the S_j and $V_{0,j}$ that, in turn, are dependent on $D_{wc,j}^2$. This means that the chamber diameter affects the virtual mass and damping of the turbine, which, in turn, increases the output captured power by each active OWC WEC. This consequently causes the reduction of the spar dynamic response.

The location of OWC is the other parameter that is investigated for its effect on the output power. However, since the interaction between OWC and spar and coupling of pitch and heave is neglected, and the governing equations and wave theory are

linear, the position of OWC cannot affect the results. This fact is confirmed in

Figure 8, in which the spar heave RAO response is the same for case studies with different distances of the OWC WECs from the spar centerline.

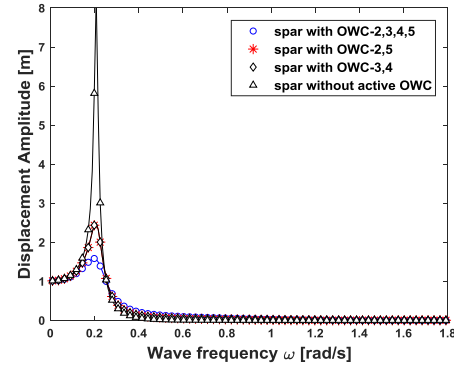


Figure 6. Effect of number of OWC WECs on heave RAO response of spar with $D_{wc} = 6 \text{ m}$.

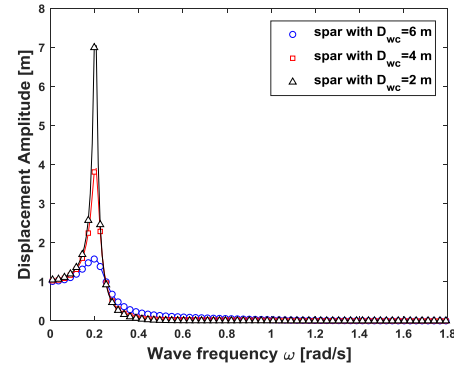


Figure 7. Effect of OWC diameter, $D_{wc} = 6, 4, 2 \text{ m}$, on heave RAO response of spar with four active OWC WECs for all cases.

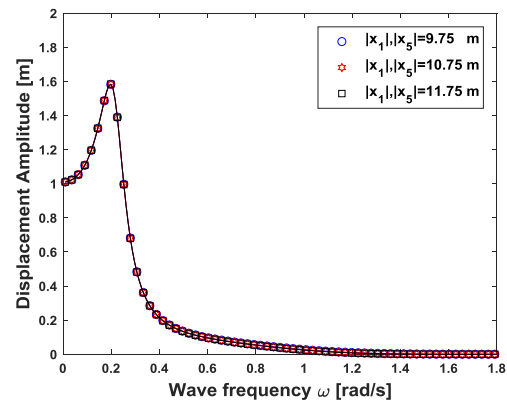


Figure 8. Effect of OWC position on heave RAO response of spar with four active OWC WECs with $D_{wc} = 6 \text{ m}$.

6. Conclusion

In the present work, an OWT with spar type platform was combined with an array of OWC WECs located in an annular arrangement around the spar. The coupled governing dynamic equations of the spar and OWC WECs were

simplified in a linear form, and a frequency domain analysis in a complex form was utilized for solving the equations. Finally, the findings from this research work are summarized below:

- 1) The large number of OWC WECs increases the generated power, and reduces the dynamic response of the spar platform.
- 2) The larger diameter of the OWC chamber increases the output power and decreases the spar heave response compared to the cases with a lower diameter.
- 3) The position of OWC WECs does not affect the output power regarding the simplified approach in which the coupling of heave and pitch does not exist.
- 4) The observed two peaks in curves of OWC power and free surface displacement versus frequency are due to the coupled motion of OWC WECs and spar platform.

7. References

- [1] A. S. Bahaj, "Generating electricity from the oceans," *Renewable and Sustainable Energy Reviews*, Vol. 15, pp. 3399-3416, 2011.
- [2] G. Iglesias and R. Carballo, "Wave energy potential along the Death Coast (Spain)," *Energy*, Vol. 34, pp. 1963-1975, 2009.
- [3] M. A. A. Farsangi and H. Zohoor, "Acoustic energy harvesting via magnetic shape memory alloys," *Journal of Physics D: Applied Physics*, Vol. 52, p. 135501, 2019.
- [4] H. Sayyaadi, H. Rostami Najafabadi, and M. A. Askari Farsangi, "Modeling and parametric studies of magnetic shape memory alloy-based energy harvester," *Journal of Intelligent Material Systems and Structures*, Vol. 29, pp. 563-573, 2018.
- [5] A. Peiffer, D. Roddier, and A. Aubault, "Design of a point absorber inside the WindFloat structure," in *International Conference on Offshore Mechanics and Arctic Engineering*, 2011, pp. 247-255.
- [6] M. J. Muliawan, M. Karimirad, and T. Moan, "Dynamic response and power performance of a combined spar-type floating wind turbine and coaxial floating wave energy converter," *Renewable energy*, Vol. 50, pp. 47-57, 2013.
- [7] E. E. Bachynski and T. Moan, "Point absorber design for a combined wind and wave energy converter on a tension-leg support structure," in *International Conference on Offshore Mechanics and Arctic Engineering*, 2013, p. V008T09A025.
- [8] J. E. Hanssen, L. Margheritini, K. O'Sullivan, P. Mayorga, I. Martinez, A. Arriaga et al., "Design and performance validation of a hybrid offshore renewable energy platform," in *2015 Tenth International Conference on Ecological Vehicles and Renewable Energies (EVER)*, 2015, pp. 1-8.
- [9] W. Chen, F. Gao, X. Meng, B. Chen, and A. Ren, "W2P: A high-power integrated generation unit for offshore wind power and ocean wave energy," *Ocean Engineering*, Vol. 128, pp. 41-47, 2016.
- [10] M. Karimirad and K. Koushan, "WindWEC: Combining wind and wave energy inspired by hywind and wavestar," in *2016 IEEE International Conference on Renewable Energy Research and Applications (ICRERA)*, 2016, pp. 96-101.
- [11] J. M. Kluger, A. H. Slocum, and T. P. Sapsis, "A first-order dynamics and cost comparison of wave energy converters combined with floating wind turbines," in *The 27th International Ocean and Polar Engineering Conference*, 2017.
- [12] Y. Wang, L. Zhang, C. Michailides, L. Wan, and W. Shi, "Hydrodynamic Response of a Combined Wind-Wave Marine Energy Structure," *Journal of Marine Science and Engineering*, Vol. 8, p. 253, 2020.
- [13] A. H. Patil and D. Karmakar, "Hydrodynamic performance of spar-type wind turbine platform combined with wave energy converter," in *Recent Trends in Civil Engineering*, ed: Springer, 2021, pp. 115-123.
- [14] C. Michailides, "Hydrodynamic Response and Produced Power of a Combined Structure Consisting of a Spar and Heaving Type Wave Energy Converters," *Energies*, Vol. 14, p. 225, 2021.
- [15] A. Peiffer and D. Roddier, "Design of an oscillating wave surge converter on the windfloat structure," in *Proceedings of the 2012 4th International Conference on Ocean Energy (ICOE)*, Dublin, Ireland, 2012, pp. 17-19.
- [16] C. Luan, C. Michailides, Z. Gao, and T. Moan, "Modeling and analysis of a 5 MW semi-submersible wind turbine combined with three flap-type wave energy converters," in *International Conference on Offshore Mechanics and Arctic Engineering*, 2014, p. V09BT09A028.
- [17] A. Aubault, M. Alves, A. n. Sarmiento, D. Roddier, and A. Peiffer, "Modeling of an oscillating water column on the floating foundation WindFloat," in *International Conference on Offshore Mechanics and Arctic Engineering*, 2011, pp. 235-246.
- [18] K. P. O'Sullivan, "Feasibility of combined wind-wave energy platforms," 2014.
- [19] C. Perez-Collazo, D. Greaves, and G. Iglesias, "Hydrodynamic response of the WEC sub-system of a novel hybrid wind-wave energy converter," *Energy Conversion and Management*, Vol. 171, pp. 307-325, 2018.

- [20] C. Perez and G. Iglesias, "Integration of wave energy converters and offshore windmills," in <http://www.icoe-conference.com>, 2012.
- [21] C. Perez-Collazo, D. Greaves, and G. Iglesias, "A novel hybrid wind-wave energy converter for jacket-frame substructures," *Energies*, Vol. 11, p. 637, 2018.
- [22] A. d. O. Falcão and P. Justino, "OWC wave energy devices with air flow control," *Ocean engineering*, Vol. 26, pp. 1275-1295, 1999.
- [23] A. J. Sarmiento and A. d. O. Falcão, "Wave generation by an oscillating surface-pressure and its application in wave-energy extraction," *Journal of Fluid Mechanics*, Vol. 150, pp. 467-485, 1985.
- [24] L. Gato and A. d. O. Falcão, "On the theory of the Wells turbine," 1984.
- [25] R. G. Dean and R. A. Dalrymple, *Water wave mechanics for engineers and scientists vol. 2: world scientific publishing company*, 1991.
- [26] S. Nallayarasu and K. Bairathi, "Hydrodynamic response of spar hulls with heave damping plate using simplified approach," *Ships and Offshore Structures*, Vol. 9, pp. 418-432, 2014.
- [27] B. Stappenbelt and P. Cooper, "Mechanical model of a floating oscillating water column wave energy conversion device," 2010.
- [28] J. N. Newman, *Marine hydrodynamics: The MIT press*, 2018.
- [29] D. Evans, "The oscillating water column wave-energy device," *IMA Journal of Applied Mathematics*, Vol. 22, pp. 423-433, 1978.
- [30] J. Jonkman, S. Butterfield, W. Musial, and G. Scott, "Definition of a 5-MW reference wind turbine for offshore system development," *National Renewable Energy Lab. (NREL), Golden, CO (United States)* 2009.
- [31] A. F. Falcão, J. C. Henriques, L. M. Gato, and R. P. Gomes, "Air turbine choice and optimization for floating oscillating-water-column wave energy converter," *Ocean engineering*, Vol. 75, pp. 148-156, 2014.
- [32] I. Simonetti, L. Cappietti, H. El Safti, and H. Oumeraci, "Numerical modelling of fixed oscillating water column wave energy conversion devices: Toward geometry hydraulic optimization," in *International Conference on Offshore Mechanics and Arctic Engineering*, 2015, p. V009T09A031.